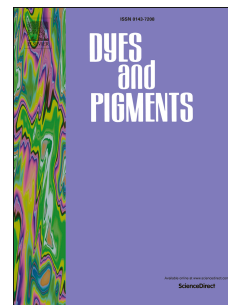


Accepted Manuscript

Extremely high pH stability for a class of heterocyclic azo dyes having the common N^2, N^6 -bis(3-methoxypropyl)pyridine-2,6-diamine coupling component

Xiao-Lei Zhao, Teng Jun, Ya-Nan Feng, Hui-Fen Qian, Wei Huang



PII: S0143-7208(17)30994-4

DOI: [10.1016/j.dyepig.2017.06.030](https://doi.org/10.1016/j.dyepig.2017.06.030)

Reference: DYPI 6051

To appear in: *Dyes and Pigments*

Received Date: 30 April 2017

Revised Date: 10 June 2017

Accepted Date: 13 June 2017

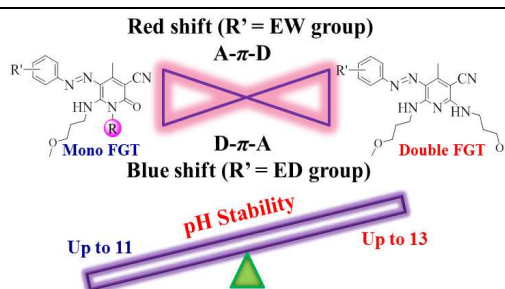
Please cite this article as: Zhao X-L, Jun T, Feng Y-N, Qian H-F, Huang W, Extremely high pH stability for a class of heterocyclic azo dyes having the common N^2, N^6 -bis(3-methoxypropyl)pyridine-2,6-diamine coupling component, *Dyes and Pigments* (2017), doi: 10.1016/j.dyepig.2017.06.030.

This is a PDF file of an unedited manuscript that has been accepted for publication. As a service to our customers we are providing this early version of the manuscript. The manuscript will undergo copyediting, typesetting, and review of the resulting proof before it is published in its final form. Please note that during the production process errors may be discovered which could affect the content, and all legal disclaimers that apply to the journal pertain.

Table of Content

Extremely high pH stability for a class of heterocyclic azo dyes having the common N^2, N^6 -bis(3-methoxypropyl)pyridine-2,6-diamine component

Xiao-Lei Zhao, Teng Jun, Ya-Nan Feng, Hui-Fen Qian, Wei Huang



Extremely high pH stability for a class of heterocyclic azo dyes having the common N^2,N^6 -bis(3-methoxypropyl)pyridine-2,6-diamine coupling component

Xiao-Lei Zhao ^a, Teng Jun ^a, Ya-Nan Feng ^b, Hui-Fen Qian ^b, Wei Huang ^{a,*}

^a *State Key Laboratory of Coordination Chemistry, Nanjing National Laboratory of Microstructures, School of Chemistry and Chemical Engineering, Nanjing University, Nanjing, Jiangsu Province, 210093, P. R. China*

^b *College of Sciences, Nanjing Tech University, Nanjing, Jiangsu Province, 210009, P. R. China*

E-mail addresses for all authors: Xiao-Lei Zhao, zhaoxiaolei2016@163.com

Teng Jun, 18648450506@163.com

Ya-Nan Feng, 1179759806@qq.com

Hui-Fen Qian, qhf@njtech.edu.cn

Wei Huang, whuang@nju.edu.cn

* Corresponding author.

E-mail address: whuang@nju.edu.cn

Abstract

A series of N^2, N^6 -bis(3-methoxypropyl)pyridine-2,6-diamine azo dyes, prepared by coupling 2,6-bis((3-methoxypropyl)amino)-4-methylnicotinonitrile and diazotized substituted anilines with distinguishable electron push-pull abilities, have been described in this paper. The new dyes undergoing double functional group transformation (FGT) show extremely high pH stability compared to corresponding mono FGT dyes, which could be ascribed to the introduction of the second 3-methoxypropylamino group forming the new pyridine-2,6-diamine backbone. It is noted that the unusual transformation from D- π -A to A- π -D system has been verified for our multi-substituted phenyl-azo-pyridine FGT products. The adjustment of electron-donating and electron-withdrawing phenyl and pyridine substituted groups narrows the discrepancy of electron push-pull capabilities for diazo and coupling components, which makes possible the transformation for roles of donor and acceptor. It is believed that the achievement of extremely high pH stability for pyridine-2,6-diamine based heterocyclic azo dyes is regarded as a useful exploration for designing new FGT modified pyridone dyes.

Keywords: Pyridone dye; Functional group transformation; UV-Vis spectrum; Push-pull substituent; pH Stability

1. Introduction

Since their discovery in the 20th century, heterocyclic disperse dyes have spurred tremendous interest among researchers because of their applications not only in the dyestuff industry [1–2] as high level-dyeing agents but also in the electronic industry including nonlinear optical devices [3], colorimetric sensors [4–5] and dye-sensitized solar cells [6]. Among them, pyridine-2,6-dione based intermediates are considered as useful coupling components in the syntheses of heterocyclic disperse dyes with a variety of diazo components [7–12], and the resultant dyes have exhibited bright hues and excellent performance on versatile fastness [13–16]. For instance, Jang *et al.* have investigated the various color range and dyeing properties for several pyridine-2,6-dione based arylazo dyes on polytrimethylene terephthalate (PTT) fabric, where the wash and light fastness were improved in comparison with C.I. Disperse Yellow 241 [17].

Regrettably, the color of these pyridine-2,6-dione based dyes fades quickly under the basic condition in the dyeing process [18–19], so the fine control of pH values should be taken into account. The possible reason is suggested to be the following: Pyridine-2,6-dione based heterocyclic dyes generally exist in the hydrazone tautomeric form under the neutral and acidic conditions, but they turn to the deprotonated azo form under the basic condition resulting in the alteration of the π -conjugated system and the color instability of the whole molecules simultaneously. The proton transfer is originated from the azo-hydrazone tautomerism in pyridine-2,6-dione based dyes, and our previous studies have demonstrated that

azo-hydrazone tautomerism can be driven by the solvent polarity, pH titration and metal-ion coordination [20–24].

To avoid the color variation problem for pyridine-2,6-dione based dyes, we have previously proposed a functional group transformation (FGT) strategy, where the acidic hydroxyl (–OH) has been transformed into a basic secondary amine (–NHCH₂CH₂CH₂OCH₃) accomplished by the configuration transformation from the hydrazone form to azo one [25]. As a result, the above-mentioned proton transfer and azo-hydrazone tautomerism have been successfully obstructed which can be verified by their increased pH stability. Actually, FGT strategy has been widely used in the antimicrobial surface modification [26], membrane modifications [27], polymer grafting and cross linking [28–29], and the introduction of reactive centers for further reactions [30]. However, there appear to be no references using FGT strategy to modify pyridine-2,6-dione precursors before us.

In this work, we have selected a special pyridine-2,6-dione precursor, i.e. 6-hydroxy-4-methyl-2-oxo-1,2-dihydropyridine-3-carbonitrile, to fulfill the double FGT for both acidic hydroxyl groups. As a result, six *N*²,*N*⁶-bis(3-methoxypropyl)pyridine-2,6-diamine based azo dyes (Scheme 1) have been produced via a 2,6-dichloropyridine intermediate, where two basic secondary amine units (–NHCH₂CH₂CH₂OCH₃) are successfully introduced. From the viewpoint of molecular design, the targeting azo dyes with *N*²,*N*⁶-bis(3-methoxypropyl)pyridine-2,6-diamine backbone are no longer pyridone derivatives, so they exhibit extremely high pH stability (1~13) evidenced by the

acid-base titration. More interesting, in the studies on structure-performance relationship for this family of double 3-methoxypropan-1-amine substituted heterocyclic azo dyes, the uncommon transformation for roles of donor and acceptor ($D-\pi-A$ and $A-\pi-D$) has been observed because of very close electron donating/withdrawing capabilities of substituted phenyl rings, which can be deduced from related electronic absorption spectral comparisons. As far as we are aware, this is the first report on N^2,N^6 -bis(3-methoxypropyl)pyridine-2,6-diamine heterocyclic azo dyes prepared from 6-hydroxy-4-methyl-2-oxo-1,2-dihydropyridine-3-carbonitrile via the FGT strategy.

2. Experimental section

2.1. Materials and physical measurements

Analytical grade reagents were purchased from commercial suppliers and used without any further purification unless otherwise stated. Intermediates **3** and **4** were prepared according to our previously reported procedure [25]. Column chromatography was carried out on silica gel (200–300 mesh). All melting points were measured without corrections. Ultraviolet-Visible (UV-Vis) spectra were recorded with a Shimadzu UV-3150 double-beam spectrophotometer using a quartz glass cell with a path length of 10 mm at room temperature (25 °C). ^1H NMR spectral measurements were performed on a Bruker DMX300 MHz NMR or a Bruker DMX400 MHz spectrometer, using chloroform-*d* (CDCl_3) as a solvent with tetramethylsilane (TMS) as the internal standard at room temperature (25 °C). Infrared

spectra in the region of 4000–500 cm^{-1} were obtained using a Nicolet FT-IR 170X spectrophotometer on KBr disks. Electrospray ionization mass spectra (ESI-MS) were recorded on a Finnigan MAT SSQ 710 mass spectrometer in a scan range of 50–500 or 50–1000 amu. Elemental analyses (EA) for C, H and N were performed on a Perkin-Elmer 1400C analyzer.

2.2.1. Preparation of compound **1** (2,6-bis((3-methoxypropyl)amino)-4-methylnicotinonitrile)

2,6-Dichloro-4-methylnicotinonitrile (1.86 g, 10.0 mmol) was added to 3-methoxypropan-1-amine (3.98 g, 44.0 mmol) under stirring, and the mixture was refluxed for 3 h. After being cooled to room temperature, 30 mL of water and 30 mL of ethyl acetate were added into the reaction solution. The aqueous layer was separated, and the ethyl acetate layer was washed twice by brine and dried with anhydrous MgSO_4 . The solvent was removed by a rotary evaporator after removing MgSO_4 , and the crude solid was recrystallized by ethyl acetate and hexane (v:v = 4:1) to give compound **1** in a yield of 2.19 g (75%). Mp: 41–43 °C. Main FT-IR absorptions (KBr pellets, ν cm^{-1}): 3376 (s), 2923 (m), 2871 (w), 2188 (vs), 1598 (vs), 1526 (s), 1356 (m) and 1119 (s). ^1H NMR (400 MHz, CDCl_3 , ppm): δ = 5.55 (s, 1H), 5.40 (t, J = 4.8 Hz, 1H), 4.98 (t, J = 5.0 Hz, 1H), 3.51 (m, 6H), 3.41 (m, 2H), 3.37 (s, 3H), 3.35 (s, 3H), 2.24 (s, 3H) and 1.86 (m, 4H). *Anal.* Calcd. For $\text{C}_{15}\text{H}_{24}\text{N}_4\text{O}_2$: C, 61.12; H, 8.27; N, 19.16%. Found: C, 60.92; H, 8.48; N, 19.02%. Positive ESI-MS in MeOH: m/z = 293.25 (100.0%), $[\text{M}+\text{H}]^+$; 315.25 (84.0%), $[\text{M}+\text{Na}]^+$. Single crystals of compound **1** suitable for X-ray diffraction measurement were obtained by slow

evaporation from a mixture of CHCl_3 and MeOH (v:v = 1:1) in air for one week.

2.2.2. Preparation of precursor
6-chloro-1,4-dimethyl-2-oxo-1,2-dihydropyridine-3-carbonitrile for preparing
compound 2

6-Hydroxy-1,4-dimethyl-2-oxo-1,2-dihydropyridine-3-carbonitrile (1.64 g, 10.00 mmol) was refluxed with phosphorus oxychloride (20 mL, 21.60 mmol) for 3 h, accompanied by the color change from yellow to red. Excess phosphorus oxychloride was then distilled under the reduced pressure, and the residue was added to ice-water (100 g) with vigorous stirring. The resulting dark red solid was filtered, dissolved in dichloromethane and washed by brine. The organic layer was dried with anhydrous Na_2SO_4 and the solvent was removed by a rotary evaporator. The crude solid was recrystallized from toluene in a yield of 1.10 g (61%). Mp: 176–178 °C. Main FT-IR absorptions (KBr pellets, $\nu \text{ cm}^{-1}$): 3074 (m), 2983 (w), 2215 (s), 1644 (vs), 1578 (s), 1533 (vs), 1447 (m) and 1198 (m). ^1H NMR (400 MHz, CDCl_3 , ppm): δ = 6.33 (s, 1H), 3.70 (s, 3H) and 2.42 (s, 3H). *Anal.* Calcd for $\text{C}_9\text{H}_9\text{ClN}_2\text{O}$: C, 52.62; H, 3.86; N, 15.34%. Found: C, 52.48; H, 3.91; N, 15.22%. Positive ESI-MS in MeOH: m/z = 183.08 (72.5%), $[\text{M}+\text{H}]^+$, 205.17 (100.0%), $[\text{M}+\text{Na}]^+$.

2.2.3. Preparation of compound 2
(6-((3-methoxypropyl)amino)-1,4-dimethyl-2-oxo-1,2-dihydropyridine-3-carbonitrile)

The synthetic procedure for compound 2 was analogous to that described for compound 3 except that

6-chloro-1,4-dimethyl-2-oxo-1,2-dihydropyridine-3-carbonitrile (1.82 g, 10.00 mmol) was used as the starting material to replace 6-chloro-1-ethyl-4-methyl-2-oxo-1,2-dihydropyridine-3-carbonitrile. Yield: 1.55 g (70%). Mp: 180–182 °C. Main FT–IR absorptions (KBr pellets, ν cm^{-1}): 3324 (vs), 2950 (w), 2877 (w), 2195 (m), 1644 (s), 1558 (vs), 1434 (m), 1237 (m) and 1119 (w). ^1H NMR (400 MHz, CDCl_3 , ppm): δ = 6.36 (s, 1H), 5.29 (s, 1H), 3.65 (t, J = 5.1 Hz, J = 10.2 Hz, 2H), 3.41 (s, 3H), 3.38 (s, 3H), 3.34 (m, 2H), 2.31 (s, 3H), 2.01 (m, 2H). *Anal.* Calcd for $\text{C}_{12}\text{H}_{17}\text{N}_3\text{O}_2$: C, 61.26; H, 7.28; N, 17.86%. Found: C, 61.12; H, 7.38; N, 17.69%. Negative ESI–MS in MeOH: m/z = 234.17 (100%), $[\text{M}-\text{H}]^+$.

2.2.4. Preparation of compound 5 *((E)-5-((4-methoxy-2-nitrophenyl)diazenyl)-2,6-bis((3-methoxypropyl)amino)-4-methylnicotinonitrile)*

4-Methoxy-2-nitroaniline (0.34 g, 2.00 mmol) was dissolved in a mixture of concentrated hydrochloric acid (1 mL) and water (1 mL) at -5 °C in an ice bath. Sodium nitrite (0.15 g, 2.20 mmol) was dissolved in water (2 mL) and added dropwise to the reaction mixture for 30 minutes under mechanical stirring. The diazonium salt solution was obtained and used for the following reaction. Compound **1** (0.58 g, 2.00 mmol) was dissolved in a methanol–water mixture (16 mL, v:v = 1:1) immersed in an ice–salt bath, and freshly prepared diazonium salt solution was added dropwise for 15 minutes under vigorous mechanical stirring (0–5 °C). After additional 3 h's stirring, the precipitate was filtered and dried after thorough washing with distilled water. The crude product was recrystallized from MeOH in a yield of

0.76 g (81%). Mp: 154–156 °C. UV–Vis in MeOH, λ_{\max} (nm) / ϵ ($\times 10^4$ L mol⁻¹ cm⁻¹) = 467 / 1.99, 312 / 1.11, 242 / 1.78. Main FT–IR absorptions (KBr pellets, ν cm⁻¹): 3363 (m), 3127 (m), 2208 (m), 1585 (vs), 1519 (m), 1401 (m), 1257 (w), 1191 (m) and 1119 (m). ¹H NMR (300 MHz, CDCl₃, ppm): δ = 10.91 (s, 1H), 7.86 (d, J = 9.1 Hz, 1H), 7.42 (d, J = 2.8 Hz, 1H), 7.17 (dd, J = 9.2, J = 2.8 Hz, 1H), 6.37 (t, J = 4.9 Hz, 1H), 3.92 (s, 3H), 3.69 (m, 4H), 3.56 (t, J = 5.6 Hz, 2H), 3.47 (t, J = 6.2 Hz, 2H), 3.41 (s, 3H), 3.33 (s, 3H), 2.71 (s, 3H) and 1.96 (m, 4H). *Anal.* Calcd. For C₂₂H₂₉N₇O₅: C, 56.04; H, 6.20; N, 20.79%. Found: C, 55.82; H, 6.38; N, 20.65%. Negative ESI–MS in MeOH: m/z = 470.33 (100.0%), [M–H]⁻.

2.2.5. Preparation of compound **6**
 ((*E*)-2,6-bis((3-methoxypropyl)amino)-4-methyl-5-((4-nitrophenyl)diazenyl)nicotinonitrile)

The synthetic procedure for compound **6** was analogous to that described for compound **5** except that 4-nitroaniline (0.28 g, 2.00 mmol) was used as the starting material to replace 4-methoxy-2-nitroaniline. Yield: 0.75 g (85%). Mp: 160–162 °C. UV–Vis in MeOH, λ_{\max} (nm) / ϵ ($\times 10^4$ L mol⁻¹ cm⁻¹) = 478 / 1.81, 310 / 1.25, 242 / 1.71. Main FT–IR absorptions (KBr pellets, ν cm⁻¹): 3127 (vs), 2877 (w), 2208 (m), 1683 (w), 1585 (s), 1401(vs), 1283 (m) and 1100 (m). ¹H NMR (300 MHz, CDCl₃, ppm): δ = 11.13 (s, 1H), 8.30 (d, J = 9.1 Hz, 2H), 7.78 (d, J = 9.1 Hz, 2H), 6.54 (t, J = 4.7 Hz, 1H), 3.71 (m, 4H), 3.58 (t, J = 5.6 Hz, 2H), 3.52 (t, J = 6.0 Hz, 2H), 3.42 (s, 3H), 3.36 (s, 3H), 2.74 (s, 3H) and 1.95 (m, 4H). *Anal.* Calcd. For C₂₁H₂₇N₇O₄: C,

57.13; H, 6.16; N, 22.21%. Found: C, 57.02; H, 6.38; N, 22.01%. Negative ESI-MS in MeOH: $m/z = 440.25$ (100.0%), $[M-H]^-$.

2.2.6. Preparation of compound **7**
 ((*E*)-2,6-bis((3-methoxypropyl)amino)-4-methyl-5-((2-nitrophenyl)diazenyl)nicotinonitrile)

The synthetic procedure for compound **7** was analogous to that described for compound **5** except that 2-nitroaniline (0.28 g, 2.00 mmol) was used as the starting material to replace 4-methoxy-2-nitroaniline. Yield: 0.74 g (84%). Mp: 125–127 °C. UV-Vis in MeOH, λ_{\max} (nm) / ϵ ($\times 10^4$ L mol⁻¹ cm⁻¹) = 461 / 2.68, 310 / 1.56, 243 / 2.28. Main FT-IR absorptions (KBr pellets, ν cm⁻¹): 3337 (s), 2923 (w), 2877 (w), 2208 (m), 1591 (vs), 1512 (m), 1283 (w), 1197 (w) and 1119 (m). ¹H NMR (400 MHz, CDCl₃, ppm): $\delta = 11.06$ (s, 1H), 7.93 (dd, $J = 8.2$ Hz, $J = 1.3$ Hz, 1H), 7.87 (dd, $J = 8.3$ Hz, $J = 1.2$ Hz, 1H), 7.61 (m, 1H), 7.37 (m, 1H), 6.49 (t, $J = 4.8$ Hz, 1H), 3.69 (m, 4H), 3.57 (t, $J = 5.6$ Hz, 2H), 3.47 (t, $J = 6.2$ Hz, 2H), 3.41 (s, 3H), 3.33 (s, 3H), 2.72 (s, 3H) and 1.96 (m, 4H). *Anal.* Calcd. For C₂₁H₂₇N₇O₄: C, 57.13; H, 6.16; N, 22.21%. Found: C, 57.00; H, 6.28; N, 22.11%. Negative ESI-MS in MeOH: $m/z = 440.25$ (100.0%), $[M-H]^-$.

2.2.7. Preparation of compound **8**
 ((*E*)-5-((2,3-dimethylphenyl)diazenyl)-2,6-bis((3-methoxypropyl)amino)-4-methylnicotinonitrile)

The synthetic procedure for compound **8** was similar to that described for compound **5** except that 2,3-dimethylaniline (0.24 g, 2.00 mmol) was used as the starting material to replace 4-methoxy-2-nitroaniline. Yield: 0.52 g (62%). Mp: 120–122 °C. UV–Vis in MeOH, λ_{\max} (nm) / ϵ ($\times 10^4$ L mol⁻¹ cm⁻¹) = 414 / 2.72, 304 / 1.31, 246 / 2.20. Main FT–IR absorptions (KBr pellets, ν cm⁻¹): 3344 (s), 2923 (w), 2863 (w), 2202 (m), 1585 (vs), 1539 (s), 1368 (w) and 1119 (m). ¹H NMR (400 MHz, CDCl₃, ppm): δ = 10.84 (s, 1H), 7.46 (m, 1H), 7.15 (m, 2H), 6.13 (t, J = 5.1 Hz, 1H), 3.66 (m, 4H), 3.55 (t, J = 5.7 Hz, 2H), 3.46 (t, J = 6.2 Hz, 2H), 3.40 (s, 3H), 3.32 (s, 3H), 2.75 (s, 3H), 2.49 (s, 3H), 2.37 (s, 3H) and 1.94(m, 4H). *Anal.* Calcd. For C₂₃H₃₂N₆O₂: C, 65.07; H, 7.60; N, 19.80%. Found: C, 64.92; H, 7.78; N, 19.59%. Negative ESI–MS in MeOH: m/z = 423.25 (100.0%), [M–H]⁻.

2.2.8. Preparation of compound **9** ((*E*)-5-((4-bromophenyl)diazenyl)-2,6-bis((3-methoxypropyl)amino)-4-methylnicotino nitrile)

The synthetic procedure for compound **9** was analogous to that described for compound **5** except that 4-bromoaniline (0.34 g, 2.00 mmol) was used as the starting material to replace 4-methoxy-2-nitroaniline. Yield: 0.76 g (80%). Mp: 103–105 °C. UV–Vis in MeOH, λ_{\max} (nm) / ϵ ($\times 10^4$ L mol⁻¹ cm⁻¹) = 435 / 2.43, 306 / 1.20, 244 / 1.58. Main FT–IR absorptions (KBr pellets, ν cm⁻¹): 3356 (s), 2926 (w), 2871 (w), 2195 (m), 1585 (vs), 1539 (s), 1381 (w) and 1112 (m). ¹H NMR (400 MHz, CDCl₃, ppm): δ = 10.89 (s, 1H), 7.56 (m, 4H), 6.23 (t, J = 5.1 Hz, 1H), 3.67 (m, 4H), 3.55 (t,

$J = 5.7$ Hz, 2H), 3.49 (t, $J = 6.0$ Hz, 2H), 3.40 (s, 3H), 3.35 (s, 3H), 2.71 (s, 3H) and 1.3 (m, 4H). *Anal.* Calcd. For $C_{21}H_{27}BrN_6O_2$: C, 53.06; H, 5.72; Br, 16.81; N, 17.68%. Found: C, 52.82; H, 5.88; N, 16.69%. Negative ESI-MS in MeOH: $m/z = 473.25$ (100.0%), $[M-H]^-$; 475.17 (96.0%), $[M+2-H]^-$.

2.2.9. Preparation of compound **10**
((E)-2,6-bis((3-methoxypropyl)amino)-4-methyl-5-(phenyldiazenyl)nicotinonitrile)

The synthetic procedure for compound **10** was analogous to that described for compound **5** except that aniline (0.19 g, 2.00 mmol) was used as the starting material to replace 4-methoxy-2-nitroaniline. Yield: 0.56 g (71%). Mp: 98–100 °C. UV-Vis in MeOH, λ_{max} (nm) / ϵ ($\times 10^4$ L mol $^{-1}$ cm $^{-1}$) = 412 / 3.39, 303 / 1.70, 245 / 2.63. Main FT-IR absorptions (KBr pellets, ν cm $^{-1}$): 3337 (s), 2930 (w), 2887 (w), 2202 (s), 1578 (vs), 1546 (vs), 1381 (m) and 1125 (m). 1H NMR (400 MHz, CDCl $_3$, ppm): $\delta = 10.96$ (s, 1H), 7.71 (dd, $J = 8.4, 1.1$ Hz, 2H), 7.45 (t, $J = 7.5$ Hz, 2H), 7.32 (t, $J = 7.3$ Hz, 1H), 6.15 (t, $J = 5.0$ Hz, 1H), 3.68 (m, 4H), 3.55 (t, $J = 5.7$ Hz, 2H), 3.50 (t, $J = 6.1$ Hz, 2H), 3.40 (s, 3H), 3.36 (s, 3H), 2.74 (s, 3H) and 1.93 (m, 4H). *Anal.* Calcd. For $C_{21}H_{28}N_6O_2$: C, 63.62; H, 7.12; N, 21.20%. Found: C, 63.42; H, 7.28; N, 19.99%. Negative ESI-MS in MeOH: $m/z = 395.25$ (100.0%), $[M-H]^-$.

2.2.10. Preparation of compound **11**
((E)-5-((4-methoxy-2-nitrophenyl)diazenyl)-6-((3-methoxypropyl)amino)-1,4-dimethyl-2-oxo-1,2-dihydropyridine-3-carbonitrile)

The synthetic procedure for compound **11** was analogous to that described for compound **5** except that compound **2** (0.47 g, 2.00 mmol) was used as the starting material to replace compound **1**. Yield: 0.51 g (61%). Mp: 170–172 °C. UV–Vis in MeOH, λ_{\max} (nm) / ϵ ($\times 10^4$ L mol⁻¹ cm⁻¹) = 453 / 1.01, 330 / 0.51, 240 / 0.65. Main FT–IR absorptions (KBr pellets, ν cm⁻¹): 3324 (m), 2877 (w), 2818 (w), 2202 (m), 1651 (s), 1565 (vs), 1434 (m), 1283 (w) and 1112 (m). ¹H NMR (300 MHz, CDCl₃, ppm): δ = 12.45 (s, 1H), 7.84 (d, J = 9.2 Hz, 1H), 7.43 (d, J = 2.8 Hz, 1H), 7.21 (dd, J = 9.2 Hz, J = 2.8 Hz, 1H), 3.93 (s, 3H), 3.76 (m, 2H), 3.61 (s, 3H), 3.35 (t, J = 5.6 Hz, 2H), 3.22 (s, 3H), 2.72 (s, 3H) and 1.99 (m, 2H). *Anal.* Calcd. For C₁₉H₂₂N₆O₅: C, 55.07; H, 5.35; N, 20.28%. Found: C, 54.82; H, 5.48; N, 19.99%. Negative ESI–MS in MeOH: m/z = 412.92 (100.0%), [M–H]⁻. Single crystals of compound **11** suitable for X–ray diffraction measurement were obtained by slow evaporation of a mixture of CHCl₃ and MeOH (v:v = 1:1) in air for one week.

2.2.11. Preparation of compound **12**

((E)-1-ethyl-5-((4-methoxy-2-nitrophenyl)diazenyl)-6-((3-methoxypropyl)amino)-4-methyl-2-oxo-1,2-dihydropyridine-3-carbonitrile)

The synthetic procedure for compound **12** was analogous to that described for compound **11** except that compound **3** (0.50 g, 2.00 mmol) was used as the starting material to replace compound **2**. Yield: 0.58 g (68%). Mp: 166–168 °C. UV–Vis in MeOH, λ_{\max} (nm) / ϵ ($\times 10^4$ L mol⁻¹ cm⁻¹) = 453 / 1.55, 347 / 0.78, 241 / 1.01. Main FT–IR absorptions (KBr pellets, ν cm⁻¹): 3120 (vs), 2825 (w), 2818 (w), 2208 (m),

1664 (s), 1565 (s), 1408 (vs), 1270 (m), 1204 (m) and 1112 (m). ^1H NMR (400 MHz, CDCl_3 , ppm): δ = 12.96 (s, 1H), 7.82 (d, J = 9.1 Hz, 1H), 7.43 (d, J = 2.8 Hz, 1H), 7.21 (dd, J = 9.1 Hz, J = 2.8 Hz, 1H), 4.22 (m, 2H), 3.93 (s, 3H), 3.79 (m, 2H), 3.40 (t, J = 5.6 Hz, 2H), 3.26 (s, 3H), 2.70 (s, 3H), 2.02 (m, 2H) and 1.42 (t, J = 7.0 Hz, 3H). *Anal.* Calcd. For $\text{C}_{20}\text{H}_{24}\text{N}_6\text{O}_5$: C, 56.07; H, 5.65; N, 19.62%. Found: C, 55.82; H, 5.88; N, 19.49%. Negative ESI-MS in MeOH: m/z = 426.83 (100.0%), $[\text{M}-\text{H}]^-$.

2.2.12. Preparation of compound **13**

((E)-1-(3-isopropoxypropyl)-5-((4-methoxy-2-nitrophenyl)diazenyl)-6-((3-methoxypropyl)amino)-4-methyl-2-oxo-1,2-dihydropyridine-3-carbonitrile)

The synthetic procedure for compound **13** was analogous to that described for compound **11** except that compound **3** (0.64 g, 2.00 mmol) was used as the starting material to replace compound **1**. Yield: 0.75 g (75%). Mp: 131–133 °C. UV-Vis in MeOH, λ_{max} (nm) / ϵ ($\times 10^4$ L mol $^{-1}$ cm $^{-1}$) = 454 / 1.66, 352 / 0.84, 243 / 1.08. Main FT-IR absorptions (KBr pellets, ν cm $^{-1}$): 3107 (w), 2970 (w), 2930 (w), 2864 (w), 2208 (m), 1664 (vs), 1565 (vs), 1278 (s), 1198 (s) and 1119 (m). ^1H NMR (300 MHz, CDCl_3 , ppm): δ = 12.88 (s, 1H), 7.81 (d, J = 9.1 Hz, 1H), 7.42 (d, J = 2.7 Hz, 1H), 7.20 (dd, J = 9.1 Hz, J = 2.8 Hz, 1H), 4.29 (t, J = 7.1 Hz, 2H), 3.92 (s, 3H), 3.82 (m, 2H), 3.50 (m, 1H), 3.40 (m, 4H), 3.23 (s, 3H), 2.70 (s, 3H), 2.00 (m, 4H) and 1.09 (d, J = 6.1 Hz, 6H). *Anal.* Calcd. For $\text{C}_{24}\text{H}_{32}\text{N}_6\text{O}_6$: C, 57.59; H, 6.44; N, 16.79%. Found: C, 57.39; H, 6.64; N, 16.59%. Negative ESI-MS in MeOH: m/z = 498.92 (100.0%), $[\text{M}-\text{H}]^-$. Single crystals of compound **13** suitable for X-ray diffraction measurement

were obtained by slow evaporation of a mixture of CHCl_3 and MeOH (v:v = 1:1) in air for one week.

2.2.18. X-ray data collection and solution

Single-crystal samples of **1**, **11** and **13** were covered with glue and were mounted on glass fibers for data collection on a Bruker SMART 1K CCD area detector at 291(2) K, using graphite mono-chromated Mo $K\alpha$ radiation ($\lambda = 0.71073 \text{ \AA}$). The collected data were reduced by using the program SAINT [31] and empirical absorption corrections were done by SADABS [32] program. The crystal systems were determined by Laue symmetry and the space groups were assigned on the basis of systematic absences by using XPREP. The structures were solved by direct method and refined by least-squares method. All non-hydrogen atoms were refined on F^2 by full-matrix least-squares procedure using anisotropic displacement parameters. The hydrogen atom (H3) bonded to the nitrogen atom of 3-methoxypropylamino moiety in compound **11** was located in the difference Fourier synthesis and refined isotropically. All the other hydrogen atoms were inserted in the calculated positions assigned fixed isotropic thermal parameters at 1.2 times of the equivalent isotropic U of the atoms to which they are attached (1.5 times for the methyl groups) and allowed to ride on their respective parent atoms. In the case of compound **1**, the solvent molecules are highly disordered, and attempts to locate and refine the solvent peaks were unsuccessful. So contributions to scattering due to these solvent molecules were removed using the *SQUEEZE* routine of *PLATON*. The

structure was then refined again using the data generated. The contents of the solvent region were not represented in the unit cell contents in the crystal data. The carbon atoms (C7, C8 in compound **11** and C62 in compound **13**) were refined as the disordered mode with the site occupancy factors as 0.717(6):0.283(6) and 0.796(7):0.204(7), respectively. All calculations were carried out on a PC with the SHELXTL [33] PC program package and molecular graphics were drawn by using XSELL, Diamond and ChemBioDraw software. Details of the data collection and refinement results for **1**, **11** and **13** are listed in Table 2. Selected bond distances and bond angles are given in Table S11, while the hydrogen bonding interactions are listed in Table 3.

3. Results and discussion

3.1. Syntheses and spectral characterizations

The introduction of functional groups into the pyridone moieties is regarded as an essential method for designing new library of heterocyclic dyes. As shown in Scheme 1, FGT strategy was used to prepare a new type of N^2,N^6 -bis(3-methoxypropyl)pyridine-2,6-diamine azo dyes **5–10**, where the two acidic hydroxylic groups of 6-hydroxypyridin-2(1H)-one precursor were successfully replaced by 3-methoxypropan-1-amine via a 2,6-dichloropyridine intermediate (Scheme S11) prior to the coupling reactions. In addition, three new 6-(3-methoxypropylamino)pyridin-2-one based dyes **11–13** with different pyridine *N*-substituted tails were synthesized as the structural analogues of

N^2,N^6 -bis(3-methoxypropyl)pyridine-2,6-diamine dye **5** for comparisons (Scheme 1), where the same 4-methoxy-2-nitroaniline diazo component was adopted with distinguishable electron-pushing ($-OCH_3$) and electron-pulling ($-NO_2$) groups simultaneously.

In our experiments, the common coupling component of N^2,N^6 -bis(3-methoxypropyl)pyridine-2,6-diamine based dyes **5–10**, i.e. 2,6-bis((3-methoxypropyl)amino)-4-methylnicotinonitrile (**1**), was synthesized from 2,6-dichloro-4-methylnicotinonitrile according to double nucleophilic substitutions. Similarly, mono 3-methoxypropan-1-amine substituted intermediate **2** was prepared from a new precursor of 6-chloro-1,4-dimethyl-2-oxo-1,2-dihydropyridine-3-carbonitrile. Compound **1** was used for the following diazo reactions with a variety of arylazo components (4-methoxy-2-nitroaniline, 4-nitroaniline, 2-nitroaniline, 2,3-dimethylaniline, 4-bromoaniline and aniline) to yield N^2,N^6 -bis(3-methoxypropyl)pyridine-2,6-diamine based dyes **5–10**. In addition, compound **2** was coupled with the diazo salt of 4-methoxy-2-nitroaniline to access 6-(3-methoxypropylamino)pyridin-2-one based dye **11** for comparison, together with two structural analogs of **12** and **13**.

It is noted that the yields of N^2,N^6 -bis(3-methoxypropyl)pyridine-2,6-diamine dyes are generally higher than those of 6-(3-methoxypropylamino)pyridin-2-one based dyes because of the better solubility and facile post-treatment of the former ones. Further solubility data of **5–13** and five previously reported 6-(3-methoxypropylamino)pyridin-2-one modified azo dyes **6a–10a** with the same

phenyl substituents reveal the obvious increase of solubility for compounds with multiple long alkyl chains in the pyridine rings (Table 1). However, the improvement of solubility of one compound sometimes means the decrease of crystallinity, so the attempts to access single-crystal structures for double 3-methoxypropan-1-amine substituted dyes **5–10** are unsuccessful. Instead, two 6-(3-methoxypropylamino)pyridin-2-one based dyes **11** and **13** are finally characterized by X-ray diffraction, together with a double 3-methoxypropan-1-amine substituted intermediate **1**.

In FT-IR spectra, the N-H stretching vibration is found as one single peak in the cases of **1** (3376 cm^{-1}) and **2** (3324 cm^{-1}), respectively, indicative of successful hydroxyl substitution by 3-methoxypropan-1-amine. In addition, the disappearance of C=O stretching vibration at 1644 cm^{-1} in compound **1** could further confirm the successful reaction between 2,6-dichloro-4-methylnicotinonitrile and 3-methoxypropan-1-amine. Similarly, the C=O stretching vibration in compounds **5–10** disappears and one strong single peak at $1578\text{--}1591\text{ cm}^{-1}$ can be observed, suggesting the formation of N=N structure. In contrast, the C=O stretching vibration in 6-(3-methoxypropylamino)pyridin-2-one modified dyes **11–13** emerges at $1644\text{--}1664\text{ cm}^{-1}$. Additionally, typical absorptions corresponding to the C≡N stretching vibration in all compounds **1–13** are located at $2201\text{--}2225\text{ cm}^{-1}$.

In their ^1H NMR spectra, the new peak at $12.45\text{--}12.96\text{ ppm}$ after FGT is assigned as the pyridyl secondary amine proton in compounds **11–13** [25]. In contrast, the two secondary amine hydrogen atoms in azo dyes **5–10** display high-field shifts to

different extents. One is in the range of 6.13–6.54 ppm ascribed to the NH proton adjacent the azo unit, and the other close to the cyano group falls within 10.84–11.13 ppm. This phenomenon demonstrates the alterations of chemical environments after mono and double 3-methoxypropan-1-amine substitution. Moreover, ESI–MS spectral approach is proved to be effective in analyzing the molecular structures of our azo dyes, where the molecular-ion peak for every compound appears undoubtedly with 100% abundance in methanol.

Generally speaking, the variations of dye structures through FGT strategy would lead to the shifts of molecular energy levels, which could be reflected by their UV–Vis electronic absorption spectra. Thus, the electronic spectra of *N*²,*N*⁶-bis(3-methoxypropyl)pyridine-2,6-diamine based dyes **5–10** and 6-(3-methoxypropylamino)pyridin-2-one modified dyes **11–13** have been determined in methanol for comparisons. As we have mentioned in our previous studies [25,34], the alteration of pyridine *N*-substituted tails with slight discrepancy in the electron withdrawing/donating capabilities would not significantly impact the π -conjugated system of the whole dye molecule. The UV–Vis spectra of azo dyes **11–13** are very similar and only dye **11** is selected as a representative to plot with dyes **5–10** for clarity (Fig. 1). Instead, dyes **12–13** have been moved to the Supporting Information as Fig. SI37. All our mono and double FGT products dyes **5–13** and **6a–10a** [25] can be divided into two categories depending on the phenyl substituents. Namely dyes **5–7**, **9**, **11–13**, **6a**, **7a** and **9a** bearing the electron-withdrawing 4-methoxy-2-nitroaniline, 4-nitroaniline, 2-nitroaniline and 4-bromoaniline moieties

and dyes **8**, **10**, **8a** and **10a** having the electron-donating 2,3-dimethylaniline and aniline moieties. By comparing the mono and double FGT products, it is found that different bathochromic shifts (14 nm from **11–13** to **5**, 15 nm from **6a** to **6**, 15 nm from **7a** to **7** and 4 nm from **9a** to **9**) and hypsochromic shifts (11 nm from **8a** to **8** and 6 nm from **10a** to **10**) can be observed for the afore-mentioned two classes of dyes, as can be seen in Table 1.

On the other hand, further inspections of the λ_{\max} values for double FGT products reveal that the position of λ_{\max} is strongly relied on the nature of the electron push-pull abilities of phenyl substituents. In comparison with the λ_{\max} peak of dye **10** centered at 412 nm, introduction of two additional electron-donating methyl groups in **8** leads to a slight hypsochromic shift of 2 nm, whereas implanting of the electron-withdrawing groups produce strong bathochromic shifts of 23~66 nm for **5–7** and **9** (Table 1). In addition, the same electron push-pull tendency is observed for all the mono FGT products **11** and **6a–10a**. With regard to four 4-methoxy-2-nitroaniline based dyes (**5** and **11–13**), the UV–Vis spectra imply that contribution of the electron-withdrawing nitro group overwhelms that of the electron-donating methoxyl group in the phenyl ring.

It should be pointed out that the variations of UV–Vis spectra for all the mono and double FGT products can be elucidated by the formation of different D– π –A and A– π –D system depending on the introduced phenyl substituents with distinguishable electron-donating and electron-withdrawing capabilities. In general, as for non-functionized aryl pyridone dyes with typical D– π –A system, the introduction of

an electron-sufficient group at the phenyl ring would induce a bathochromic shift, while the implanting of an electron-deficient one would cause a hypsochromic shift [35–36]. The same phenomenon has been observed in the cases of **8**, **8a**, **10** and **10a** with the electron-donating 2,3-dimethylaniline and aniline diazo components. However, it is not the case for all the other azo dyes with electron-withdrawing substituents. This aberrant behavior is suggested to be explicated by the transformation from D- π -A to A- π -D system for our multi-substituted phenyl-azo-pyridine skeleton. On the one hand, introducing the electron-withdrawing substituents at the phenyl ring weakens the electron density of donor. On the other hand, implanting the electron-donating secondary amine into the pyridine unit via FGT strategy strengthens the electron density of acceptor. It is therefore reasonably understood that the balance of close electron push-pull capabilities for both donor and acceptor in our compounds is responsible for the uncommon transformation from D- π -A to A- π -D system. Actually, we have tried to check the literature on this kind of transformation but we are not successful yet. We think the main reason may be the difficulties in finding a suitable example where similar electron push-pull capabilities for both donor and acceptor are present and different substituent effects are investigated simultaneously.

What impact on the pH stability can be brought for N^2, N^6 -bis(3-methoxypropyl)pyridine-2,6-diamine backbone after double FGT? To gain a better insight on the effects of pH stability, acid-base titration has been done for N^2, N^6 -bis(3-methoxypropyl)pyridine-2,6-diamine based dyes and our

experimental results demonstrate that double FGT products have extremely high pH stability in comparison with 6-(3-methoxypropylamino)pyridin-2-one based azo dyes. For example, a comparative plot for a pair of double and mono FGT products with the same 4-methoxy-2-nitroaniline diazo component (**5** and **11**) indicates that they both have high pH stability and the former reaches an extremely high value of 13 (Fig. 2). Similarly, compared with our previous prepared 6-(3-methoxypropylamino)pyridin-2-one dyes **8a** and **9a** [25], their counterparts **8** and **9** can keep stable in a wider pH range of 0.44~13.09 and 0.45~13.23 (Fig. 3). It is no doubt that the replacement of the second carbonyl group in 6-hydroxy-4-methyl-2-oxo-1,2-dihydropyridine-3-carbonitrile by the basic secondary amine unit can further enhance the pH stability for resultant double FGT dyes.

3.2. Structural descriptions of compounds **1**, **11** and **13**

As we have mentioned above, the solubility of one compound is closely related to its crystallinity. In this paper, only two single-crystal structures of mono FGT dyes **11** and **13** have been finally obtained on account of their worse solubility but better crystallinity, together with one double 3-methoxypropan-1-amine substituted intermediate **1**. X-ray single-crystal diffraction analyses reveal that all the non-hydrogen atoms in compound **11** except the 3-methoxypropylamino tail are ideally coplanar with the ZERO dihedral angle between the phenyl (A) and pyridine (B) rings, as can be seen in Fig. 4. In contrast, the dihedral angles between rings A

and B vary from 1.4(2) to 12.6(2)^o for four crystallographically independent molecules in the asymmetric unit of compound **13**, which could be ascribed to the steric hindrance between two adjacent long alkyl chains ($-\text{NHCH}_2\text{CH}_2\text{CH}_2\text{OCH}_3$ and $-(\text{CH}_2)_3\text{OCH}(\text{CH}_3)_2$) bonded to the pyridine ring. Strong intramolecular N-H \cdots N hydrogen bonds can be observed in **11** and **13** forming six-membered rings (Fig. 4 and Table 3), in which the H \cdots A distances are in a range of 1.79(2)~1.93(3) Å.

Moreover, offset dimeric π - π stacking interactions are found in the crystal packing of **11** and **13**. As shown in Fig. 5, neighboring two molecules in every dimeric unit in compound **11** adopt the head-to-tail packing fashion with the centroid-to-centroid separations of 3.603(2) Å between the pyridine and phenyl rings, but no π - π stacking interactions can be found between the dimeric units. In compound **13**, effective π - π stacking interactions can only be observed among one set of molecules forming a different head-to-head dimeric packing mode (Fig. 5). The centroid-to-centroid distance between adjacent phenyl rings in every dimeric unit is calculated to be 3.617(3) Å, and all the four long alkyl chains belonging to each molecule point outside the dimeric plane to minimize the spatial crowding effects.

4. Conclusion

To extend the synthetic strategy of FGT, we have synthesized a library of double and mono 3-methoxypropan-1-amine substituted azo dyes from classical pyridine-2,6-dione hydrazone dyes with different pyridine *N-H* and *N-R* tails.

Moreover, different aniline with distinguishable electron-donating and electron-withdrawing substituents in the diazo components are introduced into double and mono FGT products, respectively, in order to better understand their structure-performance relationship. Interestingly, the uncommon transformation for roles of donor and acceptor (D- π -A and A- π -D) can be achieved for our functionalized azo dyes because of the fine tuning of electron push-pull abilities for both phenyl and pyridine rings by adopting different substituents. Comparative studies on the UV-Vis spectra of all azo dyes clearly support the formation of different D- π -A and A- π -D system according to their respective λ_{\max} values. As expected, double basic secondary amine substituted pyridine-2,6-diamine azo dyes display extremely high pH stability up to 13 owing to the replacement of the second carbonyl group. From the current study, one can see that both the FGT strategy and structure-performance relationship can throw some light on the rational design of new dyes and effective improvements of as-synthesized dyes with better dyeing performance.

Supplementary material

Tables of selected bond distances (\AA) and angles ($^{\circ}$), FT-IR, ESI-MS, ^1H NMR and UV-Vis spectra as well as synthetic route for related compounds are attached to this paper. CCDC reference numbers 1547049-1547051 for compounds **1**, **11** and **13** contain the supplementary crystallographic data for this paper. These data can be obtained free of charge at www.ccdc.cam.ac.uk/conts/retrieving.html [or from the

Cambridge Crystallographic Data Centre, 12, Union Road, Cambridge CB2 1EZ, UK;

Fax: (internat.) +44-1223/336-033; E-mail: deposit@ccdc.cam.ac.uk].

Acknowledgements

This work was financially supported by the Major State Basic Research Development Programs (No. 2013CB922101), the National Natural Science Foundation of China (No. 21171088), and the project of scientific and technological support program in Jiangsu province (No. BE2014147-2).

References

- [1] Hallas G, Choi JH, Synthesis and properties of novel aziridinyl azo dyes from 2-aminothiophenes - Part 2: Application of some disperse dyes to polyester fibres. *Dyes Pigm* 1999;40:119–29.
- [2] Weaver MA, Shuttleworth L. Heterocyclic diazo components. *Dyes Pigm* 1982;3:81–121.
- [3] Raposo MMM, Castro MCR, Belsley M, Fonseca AMC. Push pull bithiophene azo-chromophores bearing thiazole and benzothiazole acceptor moieties: Synthesis and evaluation of their redox and nonlinear optical properties. *Dyes Pigm* 2011;91:454–65.
- [4] Cheng YF, Zhang M, Yang H, Li FY, Yi T, Huang CH. Azo dyes based on 8-hydroxyquinoline benzoates: Synthesis and application as colorimetric Hg^{2+} -selective chemosensors. *Dye Pigm* 2008;76:775–83.

- [5] Kaur P, Kaur S, Mahajan A, Singh K. Highly selective colorimetric sensor for Zn^{2+} based on hetarylazo derivative. *Inorg Chem Commun* 2008;11:626–9.
- [6] Liu J, Yang XD, Islam A, Numata Y, Zhang SF, Salim NT, Chen H, Han LY, Efficient metal-free sensitizers bearing circle chain embracing pi-spacers for dye-sensitized solar cells. *J Mater Chem A* 2013;1:10889–97.
- [7] Wang P, Wang I. Photofading of azo pyridone dyes in solution. Part II. Substituent effects on the UV absorption spectra and photostability of 3-(mono- and di-substituted arylazo)-2-hydroxy-4-methyl-5-cyano-6-pyridone in N,N-dimethylformamide. *Text Res J* 1990;60:519–24.
- [8] Peng Q, Li M, Gao K, Cheng L. Hydrazone-azo tautomerism of pyridone azo dyes: Part II: Relationship between structure and pH values. *Dyes Pigm* 1991;15:263–74.
- [9] Ertan N, Eyduran F. The synthesis of some hetarylazopyridone dyes and solvent effects on their absorption spectra. *Dyes Pigm* 1995;27:313–20.
- [10] Ozbey S, Kendi E, Ertan N. Crystal structure of hydrazone form of 1-butyl-3-cyano-6-hydroxy-4-methyl-5-(2-nitrothiazolylazo)-2(1H)-pyridone. *Dyes Pigm* 1997;33:251–8.
- [11] Mijin D, Uscumlic G, Perisic-Janjic N, Valentic N. Substituent and solvent effects on the UV/vis absorption spectra of 5-(3- and 4-substituted arylazo)-4,6-dimethyl-3-cyano-2-pyridones. *Chem Phys Lett* 2006;418:223–9.
- [12] Mijin D, Baghbanzadeh M, Reidlinger C, Kappe C. The microwave-assisted synthesis of 5-arylazo-4,6-disubstituted-3-cyano-2-pyridone dyes. *Dyes Pigm*

2010;85:73–8.

- [13]Chen CC, Wang JJ. Synthesis of some pyridone azo dyes from 1-substituted 2-hydroxy-6-pyridone derivatives and their colour assessment. *Dyes Pigm* 1991;15:69–82.
- [14]Cheng LB, Chen X, Gao KY, Hu JZ. Colour and constitution of azo dyes derived from 2-thioalkyl-4,6-diaminopyrimidines and 3-cyano-1,4-dimethyl-6-hydroxy-2-pyridone as coupling component. *Dyes Pigm* 1986;7:373–88.
- [15]Metwally MA, Galil EA, Metwally A, Amer FA. New azodisperse dyes with thiazole, thiophene, pyridone and pyrazolone moiety for dyeing polyester fabrics. *Dyes Pigm* 2012;92:902–8.
- [16]Gadre JN, Periaswamy RMS, Mulay M. Synthesis of pyridone based azo disperse dyes. *Indian J Heterocycl Chem* 2006;16:43–6.
- [17]Jang HK, Doh SJ, Lee JJ. Eco-friendly dyeing of poly(trimethylene terephthalate) with temporarily solubilized azo disperse dyes based on pyridone derivatives. *Fiber Polym* 2009;10:315–9.
- [18]Peng YX, Zhao XL, Xu D, Qian HF, Huang W. *In situ* metal-ion complexation and H₂O₂ oxidation for a pyridine-2,6-dione based disperse yellow dyes. *Dyes Pigm* 2017;136:559–68.
- [19]Peters AT, Freemant HS. *Colour chemistry: The design and synthesis of organic dyes and pigments*. London: Elsevier, 1991. [chapter1].
- [20]Xu D, Geng J, Qian HF, Chang FF, Huang W. From heterocyclic hydrazone to hydrazone-azomethine dyes: Solvent and pH induced azo-hydrazone tautomerism

- for a family of pyrazolone-based heterocyclic dyes. *Dyes Pigm* 2017;137:101–10.
- [21]Chen XC, Tao T, Wang YG, Peng YX, Huang W, Qian HF. Azo-hydrazone tautomerism observed from UV-vis spectra by pH control and metal-ion complexation for two heterocyclic disperse yellow dyes. *Dalton Trans* 2012;41:11107–15.
- [22]You W, Zhu HY, Huang W, Hu B, Fan Y, You XZ. The first observation of azo-hydrazone and cis-trans tautomerisms for Disperse Yellow dyes and their nickel(II) and copper(II) complexes. *Dalton Trans* 2010;39:7876–80.
- [23]Chen XC, Wang YG, Tao T, Geng J, Huang W, Qian HF. Two pairs of 1:2 nickel(II) and copper(II) metal-complex dyes showing the same trans configuration and azo-hydrazone transformation but different thermal properties. *Dalton Trans* 2013;42:7679–92.
- [24]Ertan N, Gurkan P. Synthesis and properties of some azo pyridone dyes and their Cu (II) complexes. *Dyes Pigm* 1997; 33:137–47.
- [25]Zhao XL, Chang FF, Feng YN, Qian HF, Huang W. Increased pH stability via functional group transformation from acidic hydroxyl to basic secondary amine for a series of pyridone based heterocyclic dyes. *Dye Pigm* 2017;140:286–96.
- [26]Mccoy CP, Cowley JF, Gorman SP, Andrews GP, Jones DS. Reduction of *Staphylococcus aureus* and *Pseudomonas aeruginosa* colonisation on PVC through covalent surface attachment of fluorinated thiols. *J Pharm Pharmacol* 2009;61:1163–9.
- [27]Corrales M, Bierbrauer K, Sacristan J, Mijangos C. Surface modification of PVC

- membranes using fluorothiophenol compounds. *Macromol Chem Phys* 2010;211:1990–8.
- [28] Coskun M, Seven P. Synthesis, characterization and investigation of dielectric properties of two-armed graft copolymers prepared with methyl methacrylate and styrene onto PVC using atom transfer radical polymerization. *React Funct Polym* 2011;71:395–401.
- [29] Singh A, Rawat MSM, Pande CS. Chemical modification and characterization of poly(vinyl chloride) by crosslinking of multifunctional amines. *J Appl Polym Sci* 2010;118:876–80.
- [30] Pawlak M, Grygolowicz-Pawlak E, Bakker E. Ferrocene bound poly(vinyl chloride) as ion to electron transducer in electrochemical ion sensors. *Anal Chem* 2010;82:6887–94.
- [31] Siemens. SAINT v4 software reference manual. Madison, Wisconsin, USA: Siemens Analytical X-Ray Systems, Inc.; 2000.
- [32] Sheldrick GM. SADABS, program for empirical absorption correction of area detector data. Germany: Univ. of Gottingen; 2000.
- [33] Siemens. SHELXTL, Version 6.10 reference manual. Madison, Wisconsin, USA: Siemens Analytical X-Ray Systems, Inc.; 2000.
- [34] Feng YN, Wang YH, Liu YH, Qian HF, Huang W. 4-Aminobenzoic acid methyl ester and pyridone based heterocyclic dyes and azo-hydrazone transformation before and after Cu(II) ion complexation. *Color Technol* 2017;133:doi: 10.1111/cote.12282.

- [35] Alimmari A, Mijin D, Vukicevic R, Bozic B, Valentic N, Vitnik V, Vitnik Z, Uscumlic G. Synthesis, structure and solvatochromic properties of some novel 5-arylaazo-6-hydroxy-4-phenyl-3-cyano-2-pyridone dyes. *Chem Cent J* 2012;6:71–8.
- [36] Alimmari A, Bozic B, Mijin D, Marinkovic A, Vukicevic R, Valentic N, Uscumlic G. Synthesis, structure and solvatochromic properties of some novel 5-arylaazo-6-hydroxy-4-(4-methoxyphenyl)-3-cyano-2-pyridone dyes: Hydrazone-azo tautomeric analysis. *Arab J Chem* 2015;8:269–78.

Table 1.

UV–Vis spectroscopic data of maximum absorption wavelengths (λ_{\max} , nm) and molar extinction coefficients (ϵ , L mol⁻¹ cm⁻¹) as well as solubility (S , mg/g) for dyes **5–13** in their methanol solutions, together with those of previously reported five 6-(3-methoxypropylamino)pyridin-2-one modified azo dyes with the same phenyl substituents labeled as **6a–10a** [25] for comparisons.

Compound	1 / 2	5 / 11	6 / 6a	7 / 7a	8 / 8a	9 / 9a	10 / 10a	12	13
$\epsilon (\times 10^4)$		1.99 / 1.00	2.81	2.68	2.72	2.43	3.39	1.55	1.66
λ_{\max}		467 / 453	478 / 462	461 / 466	414 / 425	435 / 431	412 / 418	453	454
S (mg/g)	91 / 71	2.2 / 0.7	0.9 / 0.7	1.5 / 1.1	1.5 / 0.9	1.8 / 0.7	2.0 / 1.8	1.1	1.8

Table 2. Crystal data and structural refinements for compounds **1**, **11** and **13**.

Compound	1	11	13
Empirical formula	C ₁₅ H ₂₄ N ₄ O ₂	C ₁₉ H ₂₂ N ₆ O ₅	C ₂₄ H ₃₂ N ₆ O ₆
Formula weight	292.38	414.42	500.55
Temperature / K	291(2)	291(2)	291(2)
Wavelength / Å	0.71073	0.71073	0.71073
Crystal Size (mm)	0.12×0.10×0.10	0.12×0.10×0.10	0.12×0.12×0.12
Crystal system	monoclinic	monoclinic	triclinic
Space group	<i>Cc</i>	<i>P2₁/c</i>	<i>P$\bar{1}$</i>
<i>a</i> / Å	15.692(3)	13.599(2)	17.137(1)
<i>b</i> / Å	6.970(1)	7.768(2)	17.454(1)
<i>c</i> / Å	17.153(3)	19.177(3)	18.443(1)
α / °	90	90	72.476(2)
β / °	115.571(3)	101.476(3)	85.091(2)
γ / °	90	90	71.489(2)
<i>V</i> / Å ³	1692.3(6)	1407.3(2)	4988.1(5)
<i>Z</i> / <i>D</i> _{calcd} (g / cm ³)	4 / 1.148	4 / 1.387	8 / 1.333
<i>F</i> (000)	632	872	2128
μ / mm ⁻¹	0.078	0.103	0.098
<i>h</i> _{min} / <i>h</i> _{max}	-18 / 17	-17 / 17	-20 / 22
<i>k</i> _{min} / <i>k</i> _{max}	-8 / 8	-10 / 9	-17 / 22
<i>l</i> _{min} / <i>l</i> _{max}	-20 / 20	-24 / 17	-24 / 24
Data / parameters	2545 / 191	4536 / 298	23111 / 1322
Final <i>R</i> indices	<i>R</i> ₁ = 0.0953	<i>R</i> ₁ = 0.0524	<i>R</i> ₁ = 0.0663
[<i>I</i> > 2 σ (<i>I</i>)]	<i>wR</i> ₂ = 0.2354	<i>wR</i> ₂ = 0.1421	<i>wR</i> ₂ = 0.1610
<i>R</i> indices	<i>R</i> ₁ = 0.1066	<i>R</i> ₁ = 0.0752	<i>R</i> ₁ = 0.1059
(all data)	<i>wR</i> ₂ = 0.2433	<i>wR</i> ₂ = 0.1588	<i>wR</i> ₂ = 0.1831
<i>S</i>	1.034	1.053	1.058
Max. / min. $\Delta\rho$ /e·Å ⁻³	0.393 / -0.256	0.442 / -0.398	1.036 / -0.561

$$R_1 = \frac{\sum ||F_o| - |F_c||}{\sum |F_o|}, wR_2 = \left[\frac{\sum [w(F_o^2 - F_c^2)^2]}{\sum w(F_o^2)^2} \right]^{1/2}$$

Table 3. Hydrogen bonding parameters (Å, °) in compounds **1**, **11** and **13**.

D-H...A	<i>d</i> (D-H)	<i>d</i> (H...A)	<i>d</i> (D...A)	∠DHA	Symmetry code
1					
N4-H4B...N3	0.89	2.29	3.042(1)	142	-1/2+x, 3/2-y, -1/2+z
11					
N2-H3...O3	0.90(2)	2.35(2)	3.083(3)	139(2)	
N2-H3...N5	0.90(2)	1.79(2)	2.566(3)	143(2)	
13					
N2-H2...N5	0.86	1.93	2.616(3)	136	
N8-H8...O10	0.86	2.50	3.149(3)	133	
N8-H8...N11	0.86	1.93	2.584(3)	132	
N14-H14...O16	0.86	2.59	3.294(3)	140	
N14-H14...N17	0.86	1.82	2.574(3)	146	
N20-H20A...N23	0.86	1.87	2.594(3)	140	

Figures and Scheme with captions

Fig. 1. Normalized UV–Vis absorption spectra for N^2,N^6 -bis(3-methoxypropyl)pyridine-2,6-diamine based heterocyclic azo dyes **5–10** in MeOH at room temperature, together with a 6-(3-methoxypropylamino)pyridin-2-one modified dye **11** for comparison.

Fig. 2. Comparisons of pH stability for a pair of dyes **5** (a) and **11** (b) in their MeOH solutions (6.8×10^{-5} mol/L) at room temperature.

Fig. 3. Extremely high pH stability for a pair of N^2,N^6 -bis(3-methoxypropyl)pyridine-2,6-diamine based dyes **8** (a) and **9** (b) in their MeOH solutions (6.8×10^{-5} mol/L) at room temperature.

Fig. 4. ORTEP drawings of three compounds with the atom-numbering scheme. Displacement ellipsoids are drawn at the 30% probability level and the H atoms are shown as small spheres of arbitrary radii. The dotted lines represent intramolecular hydrogen bonds.

Fig. 5. Perspective view of the π – π stacking interactions in compounds **11** and **13**.

Scheme 1. Synthetic route of heterocyclic azo dyes **5–13**.

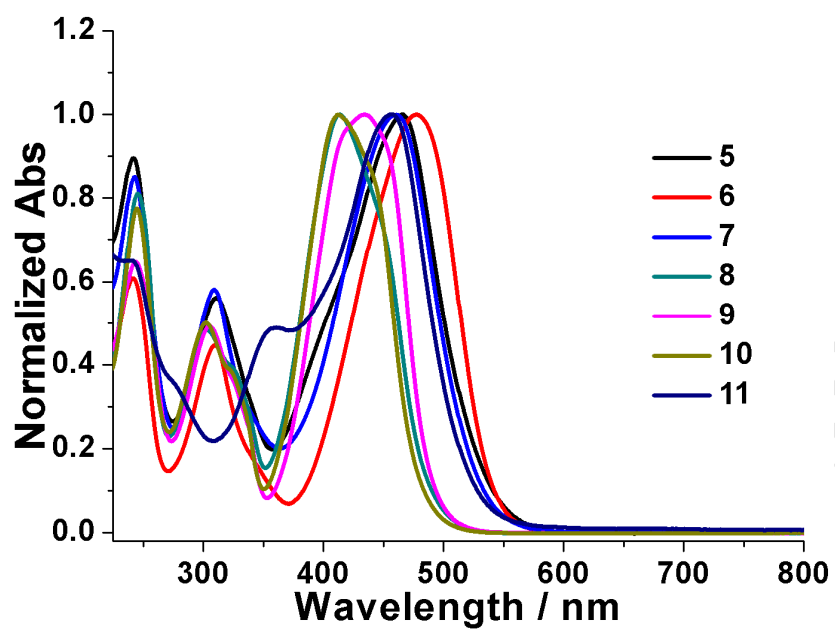


Fig. 1.

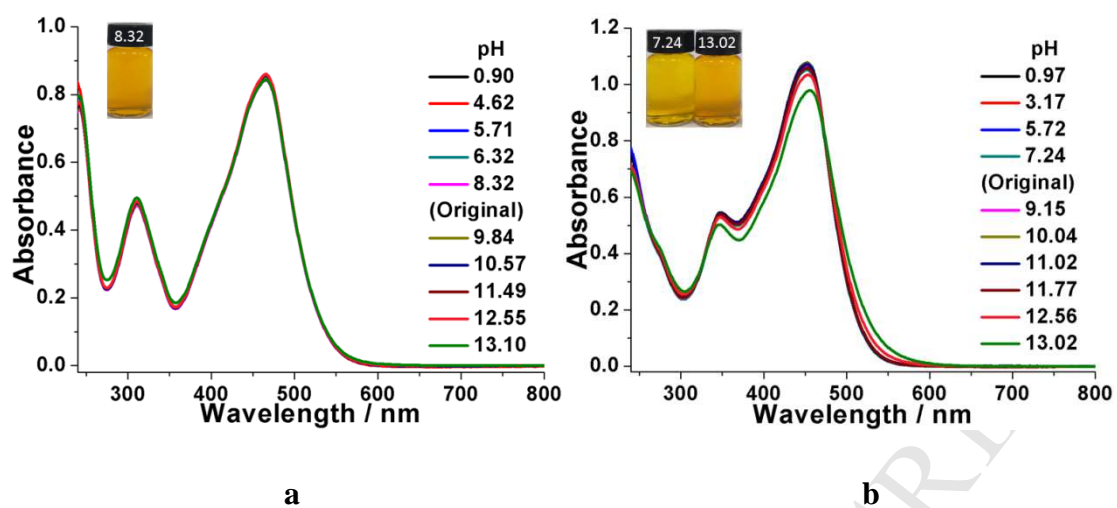


Fig. 2.

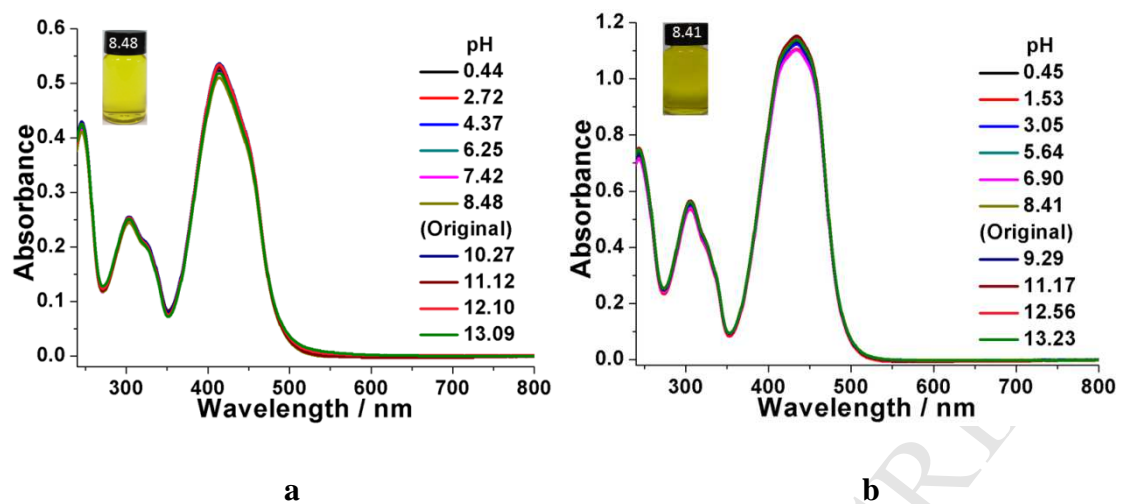


Fig. 3.

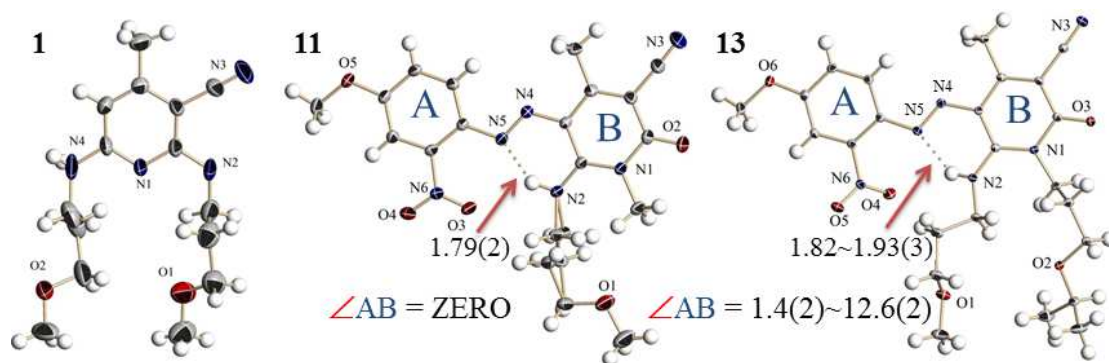


Fig. 4.

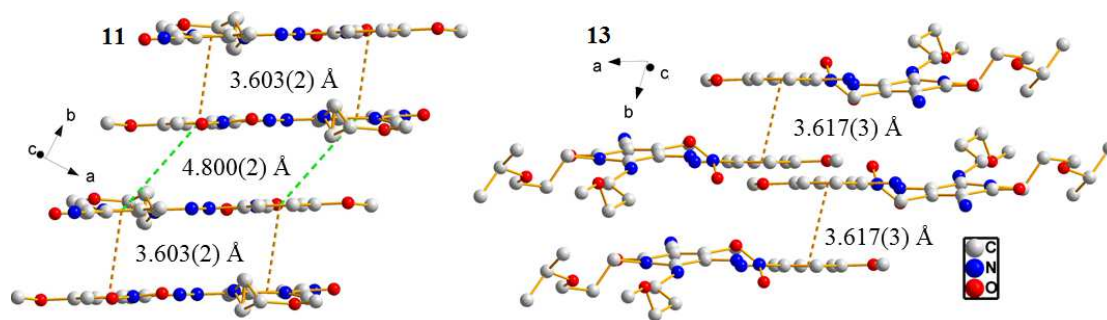
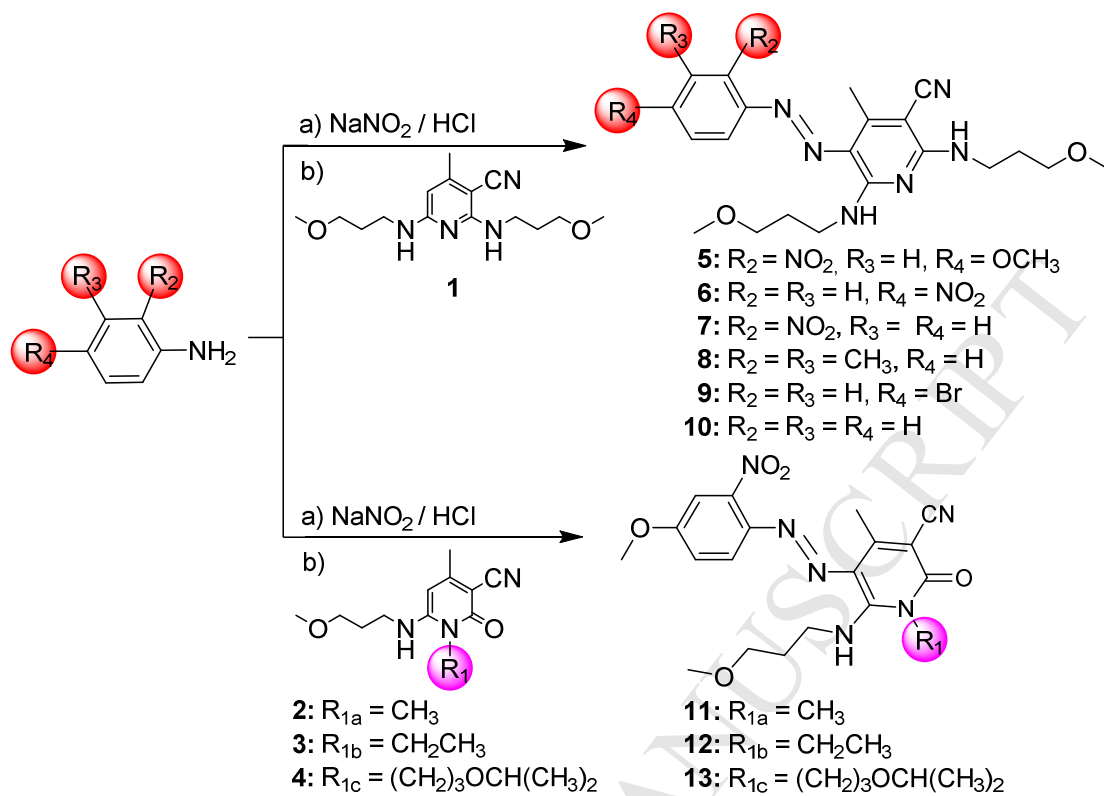


Fig. 5.



Scheme 1.

Highlights

- > Double FGT is used to modify hydroxyl groups of a *N-H* tailed pyridone precursor.
- > Six new *N*²,*N*⁶-bis(3-methoxypropyl)pyridine-2,6-diamine azo dyes are synthesized.
- > Uncommon transformation for roles of donor and acceptor is achieved.
- > All the pyridine-2,6-diamine azo dyes exhibit extremely high pH stability.